FRONTISPIECE. Test object with control points.

DR. VLADIMIR KRATKY
*National Research Council of Canada*
*Ottawa, Ont., Canada K1A 0R6*

# Digital Modeling of Limbs in Orthopaedics*

**Photogrammetry offers a reliable and objective procedure which can contribute to the automation of the production of prostheses.**

*(Abstract on page 742)*

## INTRODUCTION

TRADITIONAL methods of making limb or limb remnant models which are needed for the provision of prostheses for amputees are based on the artisan approach. The models are prepared by sculpturing or plaster casting combined with plastic moulding techniques. The main objective of modeling is to secure a good fit of the prosthesis, its shape resemblance to the original or opposite member, and a fine cosmetic appearance. The efficiency of artisan methods is relatively low because the patient and the prosthetist must meet several times and mostly manual work is involved. For a good result, the skill and experience of the prosthetist are essential. Only few large clinical centres can afford to provide services of this type.

It has been considered for a long time that a new technology can yield a better solution, more justified economically and more readily available. Such a system should be based on independent three-dimensional sensing of the shape to be reproduced, its digital modeling, and on the final reproduction with the use of computer-aided machine-tool control. The main advantage of the new system lies in

* Presented at ISP Symposium of Commission V in Washington, D.C., September 1974.

the automation and centralization of the most demanding part in the whole process of shape modeling, whereas the data gathering and final fitting of the prosthesis can be provided in several smaller centres.

Several studies are presently underway in Canada, exploring general possibilities of the new approach[3] or its technological aspects related to data sensing, processing and reproduction[2,5,9]. In these studies, the data acquisition is considered with the employment of principles of silhouette photography, silhouette video recording, analog stereophotogrammetry and shadow moiré technique.

Another study conducted at the National Research Council *(NRC)* of Canada is based on the stereophotogrammetric multiple-view approach and on the analytical solution. This article contains a technical description of the method suggested and a discussion of test results.

ABSTRACT: *Important for the production and fitting of artificial limbs in orthopaedics are the automation of the process and the shape-fidelity of the product. The potential of traditional techniques of replicating anatomical shapes by plaster casting and sculpturing is rather limited. At the present time a trend exists to employ less subjective and more technically oriented methods of three-dimensional sensing together with automatic reproduction of limb replicas by computer-controlled machines. A study conducted at the National Research Council of Canada resulted in the development and testing of a photogrammetric solution for digital modeling of limbs. A single pair of photographs is taken with the aid of two mirrors which provide a complete, simultaneous triple view of the limb. All partial stereoimages are digitized at a limited number of data points. Their coordinates are then computer-processed to yield digital output for automatic machining of the replica.*

## General Outline of the Method

A photogrammetric model reconstruction of round-shape objects, such as limbs, must be based on the availability of more than one stereopair of pictures to allow viewing of the object in its entirety. Three pairs of photographs give an adequate coverage of all details with a useful overlap and better geometric conditions than a mere minimum of two pairs. Disregarding the use of three simultaneously operated stereocameras as economically unjustified, the multiple coverage can be achieved by taking consecutive exposures from a step-wise rotating platform or of a rotating object, but the efficiency and reliability of such an approach is rather low. Another approach, in several aspects superior, requires only two simultaneous photographs, the angular range of which is extended with the use of mirrors. These are placed around the object in such a way that an unobstructed view of the full surface to be digitized is ensured. A sketch of this arrangement is shown in Figure 1. Two mirrors yield additional, reversed images of an object (Figure 2) and one composite pair of photographs taken from a fixed base can be used to reconstruct three partial models which can then be related into a uniform coordinate system.

With regard to the need of deriving digital data for the final machining of the limb replica, an analytical solution is most convenient for the photogrammetric reconstruction, and is superior to any analog approach. Even though close-range stereometric cameras mounted on a stable base should establish the geometry of the *normal* photogrammetric case, a general analytical procedure has an advantage of eliminating even the effect of any small orientation errors in the calibrated setup. For this purpose, a suitable system of auxiliary control or tie points must be established in the model space. If the coordinates of these points are determined prior to photography, the analytical solution will consist of a sequential reconstruction and subsequent unification of the partial models. If the auxiliary points are targeted but not supported by given coordinates, all three submodels must be reconstructed simultaneously with an analytical enforcement of their ties.

Only high-quality front-surface mirrors can be used in the photography, their dimensions depending on the size of the model. Considering the required accuracy of limb model-

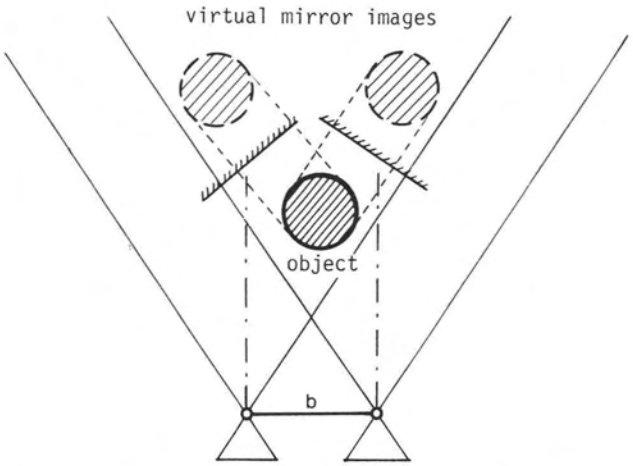


FIG. 1. Geometry of the multiple stereoview.

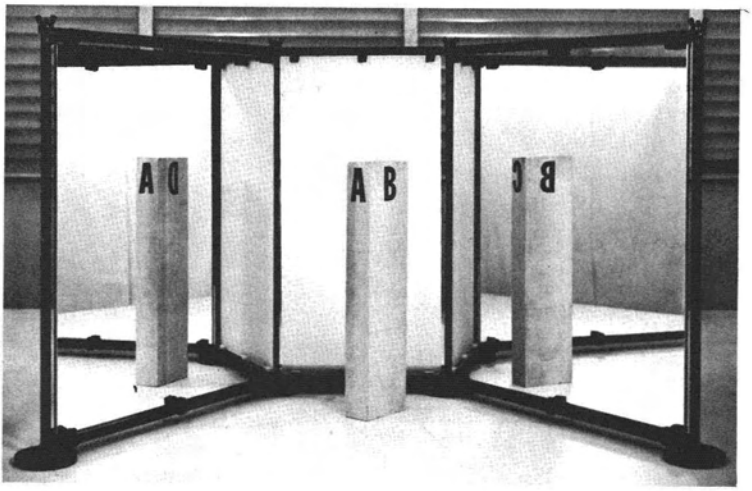

FIG. 2. Mirror-extended view.

ing, specified by an *RMS*-error of about 1 mm, and the physical dimensions of a human leg, the mirrors must be prepared by coating selected pieces of thick glass which has a plane surface with angular deviations not exceeding 30 seconds. If necessary or desirable, the geometric arrangement of the camera-mirror setup can be kept unchanged and a metric calibration of the mirror system performed. Corrections compensating for the unflatness of mirrors can be applied in the course of the analytical solution. Standard geometric conditions of the photography facilitate the computations and improve the efficiency and economy of a routine application of the method.

The analytical formulation of the prosthetic model is based on measurements performed upon a suitable, limited number of discrete points defining the surface of the limb. Two basic approaches can be considered:

- Stereocomparator digitization followed by computations in a general-purpose computer;
- Digitization and simultaneous, on-line computation of model coordinates in the analytical plotter.

If the digitization density and the point distribution were adequate, the computed model coordinates could be used directly as the input for the automated machining of the limb replica. However, this would require the use of numerically controlled machines having a capability of three-dimensional interpolation and, even then, the machining might not always be quite feasible.

A limited digitization of a minimum

number of well-distributed structural points is generally more useful because the computer off-line interpolation is more powerful as well as more efficient, and can always provide adequate data even for less sophisticated machining systems. A similar type of reasoning also seems to support the simple comparator-type of digitization rather than the analytical plotter approach. The main advantage of the analytical plotter is, of course, that it enables the operator to check on the quality of the model reconstruction during the digitization process. With the analytical plotter the digitization can also be performed in a regular pattern by guiding the floating mark in any chosen general direction, and it can be arranged in the form of continuous scanning of a series of regularly spaced data points. Theoretically, no further interpolation would then be necessary. The present *NRC* study is based on the stereocomparator approach and the other alternative is considered in the future development of the new Analytical Stereorestitutor, currently being designed at *NRC*.

The stereocomparator digitization proceeds while observing a non-oriented optical model and, therefore, it is not possible to align data points in profiles parallel to a particular coordinate system. The most efficient arrangement of measurements in all partial stereopairs is parallel to the $x$-axis in one photograph. In this instance, the model points derived from the digitized data lie in planes which form convergent bundles different for each of the three submodels. The configuration pattern of model points is irregular, to a high degree arbitrary, and not directly suitable for machining. A suitable interpolation of the data is required to ensure an appropriate density and regular configuration of data representing the final digital model. The numerical control of the machining process is then achieved in a simpler way.

Several methods are available for defining and performing the interpolation of spatially distributed data. After testing, a preference was given to the method of least-squares prediction and filtering widely used in geodesy and photogrammetry[6,7]. One of the reasons for this choice was the method's relatively simple control of smoothing given data. Another reason was that the density of the final detailed interpolation could be easily modified maintaining the set of parameters previously derived from the digitized data.

A typical and, for the interpolation, important feature of limb modeling is that the object is always represented by an enclosed surface of a cylindrical or barrel-like shape. The surface of a cylinder is then a good approximation of a trend surface so important for a proper use of the prediction method. An interpolation procedure modified to this effect yields a very stable solution with the conditions being better in the equatorial direction than in the meridional direction where the solution suffers from the well-known edge effect.

## Data Acquisition

Several commercially available close-range stereometric cameras are well suited for the purpose of limb modeling. For practical reasons, however, the *NRC* experiments were conducted using an adapted system. Two single photogrammetric cameras equipped with lenses of 157 mm focal length and using 10 × 15-cm glass plates were mounted on a rigid metal base which could be leveled and rotated on a tripod. The cameras were modified to allow for close-range focusing. The elements of interior orientation were determined with the use of a laboratory target field by means of a modified analytical resection of photographs.

As illustrated in Figure 2 and Frontispiece, two aluminum-coated, front-surface mirrors were mounted into individual metal frames linked together with a central part carrying a frosted glass to improve the illumination of the back side of the leg. The mirrors are made out of selected pieces of flat glass one-fourth-inch-thick 50 × 45 cm in size, and their mounts are adjustable to provide a suitable angle for the multiple stereoview. It was found that this angle should be about 120°, the photographic distance between 1.8 and 2.0 m, and the photogrammetric base 0.4 m. Under these conditions the reconstruction errors are characterized by a value of 0.6 mm if the estimated *RMS* error of the parallax measurement is around 10 $\mu$m. To avoid identification problems, the limb surface texture can be enhanced with the use of suitable macromesh stockings. The depth of field defined by the real object and its virtual mirror images could reach 0.45 m requiring a relatively small aperture, $f/32$. The tips of the auxiliary posts and centres of their narrow parts (Frontispiece) serve as control points in the solution. Their spatial coordinates are computed in an arbitrary local coordinate system from directly measured distances.

The stereopictures obtained were digitized with a Zeiss PSK-stereocomparator. Coordinates were measured at the control points and in arbitrary cross-sections of the limb, keeping $y = const.$ for all three partial stereomodels. The digitization was restricted

to a suitable number of discrete points important for the shape of the limb surface. The selection of the points was done by the operator directly during the measurements. Based on results of numerous experiments, six-to-eight cross-sections with three-to-seven data points, in each of the three stereoviews, were found to ensure an adequate and complete metric definition of the object. This would bring the total number of points somewhere between 50 to 150, depending on the size and shape of the object to be replicated.

## Model Reconstruction

In Figure 3, $\bar{X}, \bar{Y}, \bar{Z}$ are model coordinates in a basic righthanded $F$ system of the real object, whereas $\tilde{X}, \tilde{Y}, \tilde{Z}$ denote model coordinates in the mirror-reflected and, therefore, left-handed systems $L$ or $R$. All these systems are defined as terrestrial with the Z-axis vertical. The mirror reflection involves obviously a rotation $A_L$ ($A_R$) and a sign reversal of Y-coordinates. The computation of all three submodels $F$, $L$, $R$ proceeds in an auxiliary right-handed $X, Y, Z$ system defined according to the convention of aerial photogrammetry with the negative Z-axis in the direction of photography. Photocoordinates $x', y'$ are defined in the same *aerial* mode for all three stereopairs. The reconstruction of all three submodels is based on the orientation of photographs in the principal system $X, Y, Z$. Once the submodels are successfully formed they are subjected to the inverse transformations ($X \rightarrow \tilde{X}$ and $X \rightarrow \tilde{X}$) which reconstitute the final composite $F$-$L$-$R$ model in the unique coordinate system of the control.

### *Auxiliary Transformation*

Prior to the computation of individual submodels one can estimate their mutual orientation from the position of the mirrors and introduce an auxiliary transformation $\tilde{X} \rightarrow \bar{X}$ to eliminate the effect of the mirror reflection on the $L$- and $R$-systems. This is expressed by

$$\begin{pmatrix} \bar{X} \\ \bar{Y} \\ \bar{Z} \end{pmatrix} = \mathbf{T}_A \begin{pmatrix} \tilde{X} \\ \tilde{Y} \\ \tilde{Z} \end{pmatrix} = \begin{bmatrix} \cos A & \sin A & 0 \\ \sin A & -\cos A & 0 \\ 0 & 0 & 1 \end{bmatrix} \begin{pmatrix} \tilde{X} \\ \tilde{Y} \\ \tilde{Z} \end{pmatrix}. \quad (1)$$

Rotations $A_L$, $A_R$ can be expressed as functions of angles $\alpha$, $\beta$ (Figure 3)

$$A_L = 2\alpha \quad , \quad A_R = -2\beta$$

because the mirrors are set in a close-to-symmetric manner:

$$\alpha \cong \beta \cong 90° - \gamma/2$$

and finally

$$A_L = 180° - \gamma \quad , \quad A_R = \gamma - 180° = -A_L. \quad (2)$$

For the convenient arrangement of the mirrors their angle is $\gamma \cong 120°$ so that the rotations are usually defined by

$$A_L \cong -A_R \cong 60° \quad .$$

The next step consists in the conversion $\bar{X} \rightarrow X$ according to

$$\begin{pmatrix} X \\ Y \\ Z \end{pmatrix} = \begin{bmatrix} 1 & 0 & 0 \\ 0 & 0 & 1 \\ 0 & -1 & 0 \end{bmatrix} \begin{pmatrix} \bar{X} \\ \bar{Y} \\ \bar{Z} \end{pmatrix}, \quad (3)$$

which is applied to the given coordinates of control points for the basic submodel $F$. Control coordinates for the other submodels $L$ and $R$ are modified by substitution of Equation 1 into 3:

$$\begin{pmatrix} X \\ Y \\ Z \end{pmatrix} = \begin{bmatrix} \cos A & \sin A & 0 \\ 0 & 0 & 1 \\ -\sin A & \cos A & 0 \end{bmatrix} \begin{pmatrix} \tilde{X} \\ \tilde{Y} \\ \tilde{Z} \end{pmatrix}. \quad (4)$$

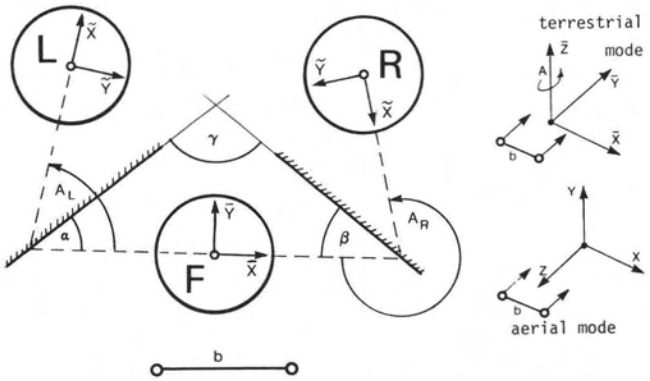


FIG. 3. Coordinate systems for the model reconstruction.

COMPUTATION OF INDIVIDUAL SUBMODELS

The elements of exterior orientation for the individual submodels are determined from the general relationship between the pictures and the model, as defined by the collinearity equations

$$F_x \equiv \Delta X\, z - \Delta Z\, x = 0$$
$$F_y \equiv \Delta Y\, z - \Delta Z\, y = 0 \qquad (5)$$

written for each projecting ray in each photograph. Here $\Delta X$, $\Delta Y$, $\Delta Z$ denote coordinates $X, Y, Z$ reduced with respect to the position of the projection centre and $x$, $y$, $z$ are defined by the orthogonal transformation of original photo coordinates $x'$, $y'$, $f$, into the system parallel with $X$, $Y$, $Z$. This is expressed as

$$\begin{pmatrix} x \\ y \\ z \end{pmatrix} = \mathbf{M} \begin{pmatrix} x' \\ y' \\ -f \end{pmatrix},$$

where $\mathbf{M}$ as a matrix of the required rotation is defined by three independent parameters $\kappa$, $\phi$, $\omega$. As the rotation is always small and defined in the first quadrant, any suitable construction of the orthogonal matrix can be employed, as described, e.g., in Reference 9.

In applying the standard least-squares solution, one can form condition equations with 12 unknown orientation parameters $\boldsymbol{g}$ for both pictures,

$$\mathbf{A}\mathbf{v} + \mathbf{B}_o\mathbf{g}_o + \mathbf{u} = 0$$

where $\boldsymbol{A}$ and $\boldsymbol{B}_o$ are matrices of partial derivatives of Equation 5, with respect to the observations $x'$, $y'$ and with respect to the orientation parameters $\boldsymbol{g}_o$ respectively; $\boldsymbol{v}$ is a vector of corrections to be applied to the observations $x'$, $y'$ and $\boldsymbol{u}$ is a vector of residuals from the functions $F_x$, $F_y$. The corresponding normal equations are

$$\mathbf{B}_o^T\mathbf{P}\mathbf{B}_o\mathbf{g}_o + \mathbf{B}_o^T\mathbf{P}\mathbf{u} = 0 \qquad (6)$$

where the weight matrix $\mathbf{P} = (\boldsymbol{A}\boldsymbol{A}^T)^{-1}$ is of a diagonal type with the weights $p_j = 1/\Delta Z_j^2$ assigned to individual rays.

If the collinearity equations are applied also to points without any control support, the unknown coordinates $X$, $Y$, $Z$ of each point extend the matrix $\mathbf{B}_o$ and vector $\mathbf{g}_o$ by additional blocks $\mathbf{B}_x$ and $\mathbf{g}_x$, respectively,

$$\mathbf{B} = [\mathbf{B}_o\ \mathbf{B}_x] \quad , \quad \mathbf{g}^T = (\mathbf{g}_o^T\,\mathbf{g}_x^T) \quad .$$

Extended normal Equations 6 can be formally simplified by the elimination of the vector

$$\mathbf{g}_x = -(\mathbf{B}_x^T\mathbf{P}\mathbf{B}_x)^{-1}\,\mathbf{B}_x^T\mathbf{P}(\mathbf{B}_o\mathbf{g}_o + \mathbf{u}) \qquad (7)$$

so that the reduced normal system is

$$\mathbf{B}_o^T\mathbf{P}_o\mathbf{B}_o\mathbf{g}_o + \mathbf{B}_o^T\mathbf{P}_o\mathbf{u} = 0 \qquad (8)$$

where

$$\mathbf{P}_o = (\mathbf{P} - \mathbf{P}\mathbf{B}_x(\mathbf{B}_x^T\mathbf{P}\mathbf{B}_x)^{-1}\mathbf{B}_x^T\mathbf{P}) \qquad (9)$$

is a matrix of pseudo-weights for quasi-observations $\boldsymbol{u}$.

An analysis of Equation 9 shows that the product $\mathbf{B}_x^T\mathbf{P}\mathbf{B}_x$, and consequently also the final matrix $\mathbf{P}_o$, have a block-diagonal form with $(4r \times 4)$-fields ${}^j\mathbf{P}_o$ computed from ${}^j\mathbf{B}_x$ (4,3) for $(j$ − th) uncontrolled model point defined by intersection of two rays.

It is evident that the reduced normal Equations 8 can be formed sequentially by the accumulation of individual contributions for all $n$ points participating in the solution

$$\underset{(12,12)}{\mathbf{B}_o^T\mathbf{P}_o\mathbf{B}_o} = \sum_{j=1}^{n} (\mathbf{B}_o^T\mathbf{P}_o\mathbf{B}_o)_j \quad ,$$

$$\underset{(12,1)}{\mathbf{B}_o^T\mathbf{P}_o\mathbf{u}} = \sum_{J=1}^{n} (\mathbf{B}_o^T\mathbf{P}_o\mathbf{u})_j \qquad (8a)$$

where ${}^j\mathbf{P}_o$ is simplified, because ${}^j\mathbf{P} = p_j\mathbf{I}$,

$$\underset{(4,4)}{{}^j\mathbf{P}_o} = p_j(\mathbf{I} - \mathbf{B}_x(\mathbf{B}_x^T\mathbf{B}_x)^{-1}\,\mathbf{B}_x^T)_j$$
$$= p_j(\mathbf{I} - \mathbf{B}_x\mathbf{B}_x^+)_j = p_j(\mathbf{I} - {}^j\mathbf{B}_x^o) \qquad (9a)$$

Here ${}^j\mathbf{B}_x^+$ is a pseudo-inverse of ${}^j\mathbf{B}_x$ and ${}^j\mathbf{B}_x^o$ is a pseudo-unit matrix formed from ${}^j\mathbf{B}_x$. The eliminated vector $\mathbf{g}_x$ of unknown model coordinates is also computed sequentially for individual points from Equation 7 when simplifying by ${}^j\mathbf{P} = p_j\mathbf{I}$

$${}^j\mathbf{g}_x = -(\mathbf{B}_x^T\mathbf{B}_x)_j^{-1}(\mathbf{B}_x^T\mathbf{B}_o\mathbf{g}_o + \mathbf{B}_x^T\mathbf{u})_j$$

or only after updating the residuals $\mathbf{u}_j$

$$\underset{(3,1)}{{}^j\mathbf{g}_x} = -\underset{(3,4)\,(4,1)}{{}^j\mathbf{B}_x^+\mathbf{u}_j} \quad . \qquad (7a)$$

For a control point given by all three coordinates $X$, $Y$, $Z$, it is obviously true that ${}^j\mathbf{B}_x = 0$ and then

$${}^j\mathbf{P}_o = {}^j\mathbf{P} \quad , \quad {}^j\mathbf{g}_x = 0$$

which is in full agreement with Equation 6. This indicates that the system of normal Equations 8 can be formally built directly in the reduced (12,12) size with the use of the same Formulas 8a and 9a for both control and intersection points. However, one must not forget to build in a programming safeguard against attempting to invert a zero matrix $(\mathbf{B}_x^T\mathbf{B}_x)_j$. In

this instance, one should either insert unity into all diagonal locations of the matrix before its inversion, or skip the inversion.

In a more general case where the control support is available only for some of the model coordinates, e.g., either for $X$, $Y$ or for $Z$, the matrix ${}^{j}\mathbf{B}_x$ is formed with zero columns in those positions corresponding to the given control coordinate. An equivalent modification is also required before inverting the product $(\mathbf{B}_x^T\mathbf{B}_x)_j$.

### SOLUTION CONSTRAINTS

In allowing the freedom of computing small orientation corrections for a stereometric setup which is not accurately calibrated for the *normal* case, there is a risk that the relatively high degree of correlation between some of the parameters will disturb some other parameters in the solution, even though these may be calibrated with sufficient accuracy. For instance, the computational weakness of separating the effect of the $X$-shift of the projection centres from that of the longitudinal tilts $\phi$ can cause an unexpected discrepancy between the computed and calibrated base components $b_x$. A formulation of suitable constraints for some adjustment parameters increases the stability of the solution and prevents a major disagreement in the expected relationship among the parameters. This is particularly important if only parts of the stereoimages can be used for the reconstruction of the model so that the equation system tends to be ill-conditioned. Obviously, this applies to our case of limb modelling.

In general, any vector of auxiliary or constraining information $\mathbf{c}$ with known stochastic properties characterized by its variance-covariance matrix $\mathbf{Q}_c$, describes some functional relationship $F_c$ among the parameters $\mathbf{g}_o$. As such, any available information of this kind can enhance the least-squares adjustment with new conditions

$$F_c(\mathbf{g}_o, \mathbf{c}) = 0$$

and contribute to the formation of normal equations. Its linearized form

$$\mathbf{A}_c\mathbf{v}_c + \mathbf{B}_c^T\mathbf{g}_o + \mathbf{u}_c = 0$$

is equivalent to pseudo-corrections $\mathbf{w}$ of the constraining functions

$$\mathbf{w}_c = \mathbf{B}_c^T\mathbf{g}_o + \mathbf{u}_c$$

with the corresponding weight matrix

$$\mathbf{P}_u = \mathbf{Q}_u^{-1} = (A_c\mathbf{Q}_c\mathbf{A}_c^T)^{-1}.$$

Here the meaning of the used notation $\boldsymbol{A}, \boldsymbol{B}, \boldsymbol{u}$ is the same as in the previous section. Accordingly, if imposing constraints on the solution, the normal Equations 8 must receive new contributions $\mathbf{B}_c^T\mathbf{P}_u\mathbf{B}_c$ and $\mathbf{B}_c^T\mathbf{P}_u\mathbf{u}_c$.

A variety of ways are available to define constraints in a close-to-normal photogrammetric situation. Conditions can be set to enforce the assignment of certain values to certain elements ($\kappa=0$, $\phi=0$, $\omega=0$) or to their combinations ($\phi_2-\phi_1=0$, $b_y=0$, etc.). At the same time, one controls the degree of urgency of the enforcement by a suitable assessment of the quality of available information in choosing or estimating the matrix $\mathbf{Q}_c$.

After extensive testing, two additional conditions were deemed appropriate to constrain the computation of submodels in the *NRC* study. They express the fact that the length of the photogrammetric base is known and can be determined and kept constant with higher confidence than other orientation elements. Furthermore, the base can be easily kept horizontal but not parallel to some chosen direction. This is true because the analytical reconstruction proceeds in a system whose orientation is determined for all three submodels only in an approximate way. Using the notation of aerial photogrammetry, the $b_x$- and $b_z$-components must conform to the given length $b$ of the base whereas $b_y$-component is considered to be zero. The respective constraint functions have a form

$$F_c \equiv \left\{ \begin{matrix} b_x^2 + b_z^2 - b^2 = 0 \\ b_y = 0 \end{matrix} \right\} \qquad (10)$$

from which the matrix $\mathbf{B}_c$ is derived with respect to some of the parameters $\mathbf{g}_o$

$$\mathbf{B}_c = \begin{bmatrix} -2b_x & 0 & -2b_z & 2b_x & 0 & 2b_z & 0 & \dots & 0 \\ 0 & -1 & 0 & 0 & 1 & 0 & 0 & \dots & 0 \end{bmatrix} \qquad (11)$$

$$\mathbf{g}_o^T = (dX_1\, dY_1\, dZ_1\, dX_2 dY_2\, dZ_2\, \kappa_1\, \dots\, \omega_2)\ .$$

Residual vector $\mathbf{u}_c$ results from Equation 10 and the stochastic potential of the constraints is represented by

$$\mathbf{Q}_c = \begin{bmatrix} 4b^2 & 0 \\ 0 & 1 \end{bmatrix} \hat{\sigma}_b^2 \qquad (12)$$

where the uncertainty of both $b$ and $b_y$ is assessed by the same variance estimate $\hat{\sigma}_b^2$.

### SIMULTANEOUS SOLUTION

The analytical reconstruction of the limb model can also be solved by a simultaneous computation of all the three submodels. In this instance the size of normal equations is

extended to 36 unknowns. The basic Formulas 7a to 9a maintain their form whereas their sizes change. The solution is also more general in that some of the intersection points can and should be chosen common to two submodels to assume a function of tie points. For these points intersected always from four rays, the size of some arrays is increased as follows:

$$ {}^{j}\mathbf{B}_X(8,3) \quad , \quad {}^{j}\mathbf{P}_o(8,8) \quad , \quad {}^{j}\mathbf{B}^{+}_X(3,8) \quad , \quad \mathbf{u}_j(8,1). $$

In the simultaneous solution, the existence of control points is not so essential as in the sequential solution, and targets placed within the model space can be used just as tie points. The model scale is then determined and automatically transferred to the model from the base constraints. In order to make the scale transfer less dependent or completely independent on the accuracy of measured image data, the estimated variance $\hat{\sigma}_b^2$ must be entered into the computations as a very small value.

## Interpolation

The method of prediction and filtering, termed also as *least-squares interpolation*, is described in numerous publications and used in connection with diverse applications. A general and very comprehensive outline of its potential in photogrammetry is given in References 6 and 8. The multisurface analysis and modeling as described, e.g., in Reference 4 is basically a variant of the prediction method based on a different geometric interpretation. It is generally recognized that the prediction method is very powerful in digital modeling.

One of the basic assumptions for a rigorous application of the prediction method is that the vector of observations **l** is composed of two independent classes of random variables — of the signal **s** with a high degree of autocorrelation, and of the random noise **r**, the components of which are absolutely correlation-free. Another assumption states that all components of **l, s, r**-vectors have zero expectations. This means that the observations to be processed should be defined with respect to the trend surface.

### Preliminary Transformation

The orthogonal coordinate system in which the digital model of a limb is defined obviously does not conform to the above assumption on expentancy. The first thing to do before attempting to interpolate is to find a suitable reference surface in relation to which the digital data should be redefined.

As far as limb modeling is concerned, the simplest standard form of a trend surface is a cylinder. A cylinder of a suitable diameter can be fitted with the model data using a least-squares solution.

This fitting is accomplished with the use of suitable rotations $\phi$, $\omega$ of the model, combined with a shift $dX$, $dY$ and with a determination of a suitable radius $R$ for the reference cylinder. This is expressed by a transformation of original $X, Y, Z$ coordinates into a new system $\overline{X}, \overline{Y}, \overline{Z}$

$$ \begin{pmatrix} \overline{X} \\ \overline{Y} \\ \overline{Z} \end{pmatrix} = \begin{pmatrix} dX \\ dY \\ 0 \end{pmatrix} + \mathbf{T}_\phi \mathbf{T}_\omega \begin{pmatrix} X \\ Y \\ Z \end{pmatrix} \qquad (13) $$

controlled by the condition

$$ F_R \equiv \overline{X}^2 + \overline{Y}^2 - R^2 = 0 \quad . \qquad (14) $$

Linearized Condition 14 leads to the system of normal equations

$$ \mathbf{B}^T\mathbf{P}\mathbf{B}\mathbf{g} + \mathbf{B}^T\mathbf{P}\mathbf{u} = 0 $$

where $\boldsymbol{u}$ are residuals for the function $F_R$, and further,

$$ \mathbf{B} = 2\begin{bmatrix} X & Y & XZ & YZ & R_o \end{bmatrix} $$

$$ \mathbf{g}^T = (dX \quad dY \quad \phi \quad \omega \quad dR) $$

$$ \mathbf{A} = \begin{bmatrix} 2X & 2Y \end{bmatrix} $$

$$ \mathbf{P} = (\mathbf{A}\mathbf{A}^T)^{-1} = (1/4R_o^2)\mathbf{I} $$

An approximate solution is satisfactory for the fitting, and an iterative refinement of parameters is not necessary. The parameters derived from the fitting are used to implement the translation and rotation of the model in accordance with Equation 13. Finally, the conversion of $\overline{X}, \overline{Y}, \overline{Z}$ into the cylindrical system of coordinates $\Theta$, $r$, $\overline{Z}$ illustrated in Figure 4, is performed

$$ \begin{aligned} \Theta &= \arctan(\overline{Y}/\overline{X}) \\ r &= (\overline{X}^2 + \overline{Y}^2)^{1/2} \quad . \end{aligned} \qquad (15) $$

### Interpolation Parameters

For the interpolation, the model is expressed in cylindrical coordinates $\Theta$, $\overline{Z}$, $dr$ after the radial distances $r$ originally computed from Equation 15 are reduced with respect to the cylindrical trend surface with radius $R = R_o + dR$. The reduced values $dr = r - R$ define the surface as a function of coordinates $\Theta$, $\overline{Z}$,

$$ dr = F(\Theta, \overline{Z}) \qquad (16) $$

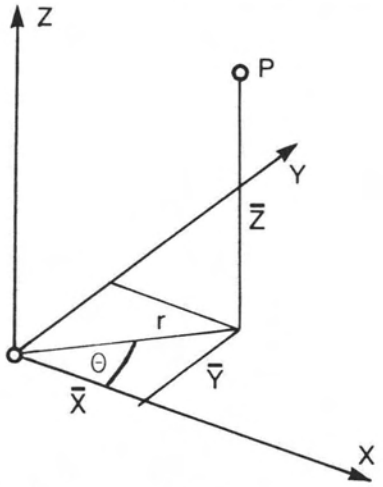


FIG. 4. System of cylindrical coordinates.

and represent the observations $\boldsymbol{l}$ in the process of interpolation.

An estimate $\hat{s}$ of the signal predicted for any location in a stochastic field from observations $\boldsymbol{l}$ is expressed by the well-known relation,[6]

$$\hat{s} = \mathbf{c}^T\mathbf{C}^{-1}\mathbf{l} \qquad (17)$$

where $\boldsymbol{c}$ is a vector of covariances between the new location and the set of all locations for observations $\boldsymbol{l}$. Similarly, $\boldsymbol{C}$ is a variance-covariance matrix of the observations. Diagonal elements in the matrix $\boldsymbol{C}$ are defined as variances $V_l$ computed from the observations $\boldsymbol{l}$; in this way they express the combined effect of both present components $s$ and $r$. All the remaining covariances in $\boldsymbol{C}$ and $\boldsymbol{c}$ are derived as covariance functions from respective distances d between pairs of related points. This relationship can be represented by the Gaussian function

$$C(d) = C_o G(d) = C_o exp\,(-kd^2) \qquad (18)$$

where $C_o$ is a magnitude of the function $C(d)$ for $d=0$ and $k$ is a coefficient controlling the spread of the Gaussian function.

In the present study, the covariance function is not derived from a numerical analysis of existing correlations among the data, but is determined *a priori* from considerations based on experience with models of this type. The coefficient $C_o$ is computed as a difference between the previously computed variance $V_l$ and estimated variance $V_r$ of random noise expected to be filtered out in the process of interpolation

$$C_o = V_l - V_r \quad . \qquad (19)$$

As for the distances $d$ between pairs of points in the limb model, these are computed on the surface of the reference cylinder according to

$$d^2 = (R\,\Delta\Theta)^2 + \Delta\bar{Z}^2 \quad .$$

The coefficient $k$ in Function 18 is derived in a way related to the average spacing interval $D$ among the observations

$$k = 0.5/D^2 \quad . \qquad (20)$$

With this substitution the Function 18 assumes the following values for different distances $d$:

| $d$ | 0 | $D$ | $2D$ | $3D$ |
|---|---|---|---|---|
| $G(d)$ | 1.00 | 0.61 | 0.14 | 0.01 |

.

It is evident that the value of the covariance drops with the distance $d$ at a suitable rate and is practically negligible beyond distances greater than $3D$.

Another modification proved also very useful. The Gaussian function can be decomposed by the substitution of $d^2 = x^2 + y^2$ as

$$G(d) = exp(-k_x x^2) \cdot exp(-k_y y^2) = G(x) \cdot G(y) \qquad (21)$$

where

$$k_x = 0.5/D_x^2 \quad , \quad k_y = 0.5/D_y^2 \quad .$$

This arrangement makes it possible to define a different spread of the Gaussian function in both basic directions $x$ and $y$ without introducing an affine transformation to the whole field of interpolation, which is otherwise necessary wherever the spacing of data points is different in $x$ and $y$.

### DETAILED INTERPOLATION

Equation 17 can be formally modified in two different ways. Substituting $\mathbf{c}^T\mathbf{C}^{-1} = \mathbf{a}^T$, the new estimate

$$\hat{s} = \mathbf{a}^T\mathbf{l} \qquad (17a)$$

is expressed as a linear function of the original observations, the coefficients $a_j$ being different for each new position. In a more practical approach the substitution

$$\mathbf{C}^{-1}\,\mathbf{l} = \mathbf{p}$$

defines parameters of the interpolation as correlates for a given configuration of $\boldsymbol{l}$ and the new estimate

$$\hat{s} = \mathbf{c}^T\mathbf{p} \qquad (17b)$$

is a linear function of these parameters. In this latter arrangement the computer storage and time requirements are lower, and the interpolation can be extended, supplemented or repeated any time later in a

new density or configuration pattern with the use of the once-computed and stored parameters $\boldsymbol{p}$.

This is quite important for the preparation of final data for the numerically controlled process of machining. The model is determined in rectangular $(\overline{X},\overline{Y},\overline{Z})$ or cylindrical $(\Theta,\overline{Z},r)$ coordinates in a regular spatial grid of an optional density. The point sequences on the model surface actually represent meridians defined at constant intervals $\Delta\Theta$ by a set of planes containing the $\overline{Z}$-axis, or parallels formed by a series of secant $\overline{X},\overline{Y}$-planes at constant intervals $\Delta\overline{Z}$. A computer-generated perspective plot shown in Figure 5 gives an insight into the data organization.

The interpolation accuracy depends on the position of the interpolated point within the field of observation points and can be estimated with the use of the law of weight propagation as demonstrated by Kraus[7]. This eventually leads to an expression for the variance of an interpolation signal $\hat{s}$

$$\sigma^2_{\hat{s}\hat{s}} = \mathbf{C}_o - \mathbf{c}^T\mathbf{C}^{-1}\mathbf{c} \qquad (22)$$

which can be computed for every new point in the course of interpolation to characterize the local quality of the interpolation.

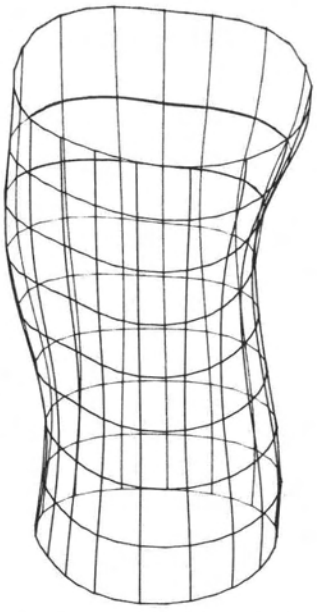

FIG. 5. Computer plot of the digital model.

## PRACTICAL RESULTS

Several experiments and practical tests were carried out at *NRC* to prove the feasibility and to assess the accuracy of the suggested solution. The tests were based on three different types of data:

- ★ Fictitious, computer-generated analytical surfaces simulating the shape of a limb,
- ★ Wooden machined model of a limb, such as in Figure 6, provided by courtesy of Prof. J. P. Duncan of University of British Columbia,
- ★ Real, live model, such as in the Frontispiece.

Three Fortran programs were developed for processing of the original digitized data. The first program solves the metric reconstruction of the composite model in the three-dimensional space. The accuracy of the reconstruction is checked by the program, the results being printed out and stored on magnetic tape for a subsequent use. A listing gives basic information on the photogrammetric setup, shows the parameter increments in the iterative solution, lists the final orientation elements, coordinates of participating points, as well as residuals in the model space (in mm) and in the photographs (in $\mu$m). The standard errors of unit weight and of computed parameters characterize the accuracy of the reconstruction. More information on the inner stability of the solution is provided by the variance-covariance matrix of the unknowns in a separate printout.

The second program is started if the quality of the preceding solution is satisfactory. A series of additional computer listings is available for checking purposes. The final condensed information on the derived digital model is punched out in cards or stored on magnetic tape. The first two lines identify the solution and its conditions whereas the rest of the printout lists model coordinates $\overline{X}$, $\overline{Y}$, $\overline{Z}$, $\Theta$, $r$ and interpolation parameters $p$ of Equation 17b associated with each individual data-point.

The last program uses the derived parameters to generate the final data-grid necessary for the computer-controlled machining process. An output contains a dense regular grid of values $r$ (in units of 0.01 mm) arranged in meridians and parallels of optional spacing in correspondence with the plot in Figure 5.

The accuracy of the interpolation depends largely on the density and on the configuration of digitized points. As mentioned above, the interpolation can be controlled by choosing the values $k_x$, $k_y$ in Equation 21 for the computation of the Gaussian function. Mainly because the model surface is enclosed in equatorial cross-sections, a change of the $k_x$-value does not affect the computation very much, yielding a stable accuracy for a reasonably wide range of changes. On the

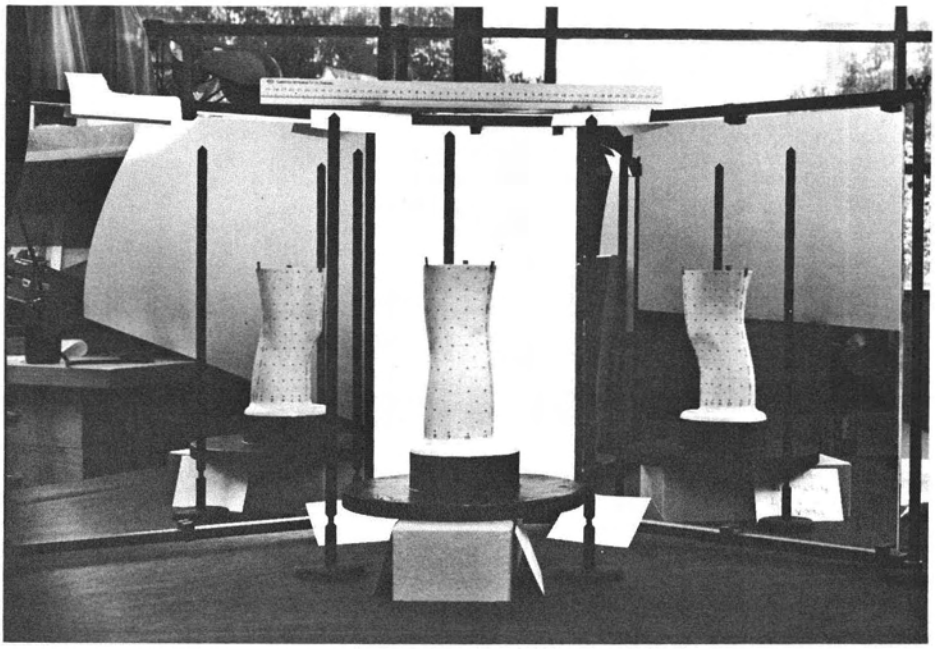

FIG. 6. Test model.

other hand, the interpolation is more sensitive to the selection of $k_y$ and clearly reflects the boundary problem in meridional cross-sections.

Any interpolation beyond the limits of the field of given data points has a tendency towards the zero level of the reference surface. In response to this, the edge of the interpolated model becomes systematically distorted in the form of a bulged rim. This is more pronounced if the spread of the $G(y)$-function is too narrow which, in general, disturbs the continuity of interpolation between given points. In the opposite situation of an excessive spread, more points participate in the solution, the covariance differences are smaller and, in the extreme, the solution may gradually become weaker and less accurate.

Table 1 illustrates the practical effect of choosing different values for $D_y$ in the computation of $k_y$ in a test model defined by 96 data points and containing 272 check points. The actual average $y$-spacing of data-points in this instance was 40 mm. The results indicate that the spread of the $G(y)$-function should be defined using $D_y$ approximately twice larger than the interval between digitized cross-sections.

With a suitable choice of the $D_y$-interval the standard error of digital limb modeling in the *NRC* experiments was tested to be always between 0.05 and 0.40 mm, for solutions supported by 100 to 50 data points. The systematic edge effect was further suppressed with the aid of denser spacing of the first two cross-sections at the top and at the bottom of the model.

TABLE 1. INTERPOLATION ACCURACY

| $D_y$ | 50 mm | 60 | 70 | 80 | 90 mm |
|---|---|---|---|---|---|
| $\sigma_r$ | 0.26 mm | 0.14 | 0.08 | 0.07 | 0.22 mm |
| $\max\lvert\epsilon_r\rvert$ | 0.46 mm | 0.26 | 0.16 | 0.14 | 0.30 mm |

## CONCLUSION

Photogrammetric digital modeling is a reliable and objective procedure which can be used to define the true shape of a human limb, so providing metric data needed for an automated production of prostheses.

## REFERENCES

1. Abdelmalek, N. N., "The Pseudo-Inverse of a Matrix and the Linear Least Squares Problem", *Lectures in Numerical Analysis*, National Research Council, Ottawa 1973.
2. Duncan, J. P., Patterson, F. P., Foort, J., "Three Dimensional Shape-Sensing and Reproduction of Limbs and Limb Remnants", Interim Report, University of British Columbia, Vancouver 1973.
3. Foort, J., Personal Communication.
4. Hardy, R. L., "Geodetic Applications of Multiquadric Analysis", *Allgemeine Vermessungs-Nachrichten*, 79(10), 1972.

5. Johnson, E. W., McGregor, I., "Three Dimensional Shape-Sensing at Mechanical Engineering Department of University of Calgary", Appendix to Reference 2.
6. Kraus, K., Mikhail, E. M., "Linear Least-Squares Interpolation", *Photogrammetric Engineering*, 38(6), 1972.
7. Kraus, K., "Untersuchung zur Genauigkeit der Interpolation nach kleinsten Quadraten", Zeitschrift für Vermessungswesen 99(5), 1974.
8. Moritz, H., "Neuere Ausgleichungs- und Prädiktionsverfahren", *Zeitschrift für Vermessungswesen*, 98(4), 1973.
9. Schut, G. H., "Construction of Orthogonal Matrices and their Application in Analytical Photogrammetry', *Photogrammetria*, 15(4), 1958-1959.
10. Thornton-Trump, A. B., "Three-Dimensional Shape Sensing Using Splines", Presented to the Workshop on Three-Dimensional Shape Sensing in Orthopaedics, Vancouver, October 1973.

## 35th Photogrammetric Week
## Stuttgart, September 8-13, 1975

The Photogrammetric Weeks have long held a firm place in the photogrammetric community as a technical seminar for professional photogrammetrists and as an international forum for the exchange of ideas. Because of the great success of the 34th Photogrammetric Week — held for the first time in Stuttgart in 1973 — that city will again be the host for the 35th Photogrammetric Week, scheduled for the week of September 8 to 13, 1975.

The seminar will be under the scientific direction of Prof. Dr.-Ing. F. Ackermann, Stuttgart, and Dr.-Ing. H.-K. Meier, Oberkochen. It will include a review of the present status of photogrammetric techniques followed by an overview of the most important trends in development. Some 18 lectures by an international group of experts will be devoted to

- The status of photogrammetry and remote sensing
- Image acquisition and processing
- Computer-supported stereoplotting

The opening sessions will include papers on new photogrammetric instruments. Simultaneous translations of the lectures in German, English, French, and Spanish will be provided. Demonstrations of and exercises on photogrammetric instruments are scheduled for three afternoons during the seminar.

Additional information may be obtained from

Universität Stuttgart
Institut für Photogrammetrie
D-7000 Stuttgart 1, Postfach 560
West Germany

or

Carl Zeiss
Surveying and Photogrammetry Division
D-7082 Oberkochen/Württ., Postfach 1369/1380
West Germany

The closing date for applications is July 15, 1975.

## Fifth Biennial Workshop —

## Color Aerial Photography in Plant Sciences and Related Fields.

*August 19-21, 1975.*

*EROS Data Center, Sioux Falls, South Dakota.*

The Workshop is sponsored by the American Society of Photogrammetry and is hosted by the Dakota Chapter of ASP and the EROS Data Center. The focus, as in past years, will be on the use of color or color-infrared photography and other remote sensing techniques in the plant sciences.

Advance registration requested.

Contact: Ms. Fredericka Simon, President
ASP, Dakota Chapter
7401 North Cliff
Sioux Falls, South Dakota 57101